phys. stat. sol. (a) **205**, No. 5, 1190–1195 (2008) / **DOI** 10.1002/pssa.200723476

physica status solidi a
www.pss-a.com
applications and materials science

Facile synthesis of large scale Er-doped ZnO flower-like structures with enhanced 1.54 μm infrared emission

Wei-Chieh Yang[1], Chun-Wen Wang[1], Jr-Hau He[2], Yu-Cheng Chang[1], Jen-Cheng Wang[2], Lih-Juann Chen[*,1], Hung-Ying Chen[3], and Shangir Gwo[3]

[1] Department of Materials Science and Engineering, National Tsing Hua University, Hsinchu 300, Taiwan
[2] Graduate Institute of Electro-Optical Engineering and Department of Electrical Engineering, National Taiwan University, Taipei 106, Taiwan
[3] Department of Physics, National Tsing Hua University, Hsinchu 300, Taiwan

Received 3 October 2007, revised 19 December 2007, accepted 20 December 2007
Published online 19 March 2008

PACS 68.37.Lp, 78.55.Et, 81.05.Ea, 81.16.Rf

[*] Corresponding author: e-mail ljchen@mx.nthu.edu.tw, Fax: (+886)3571-8328

A new strategy to introduce metallic dopant into ZnO structures by a wet chemical reaction is presented. Single-crystal Er-doped ZnO flower-like structures have been synthesized on ZnO-coated silicon substrate by a low temperature hydrothermal process. The Er-doped ZnO structures exhibit promising 1.54 μm photoluminescence emission for optoelectronic communication. The successful doping has been confirmed by the X-ray diffraction, transmission electron microscopy, X-ray photoemission spectroscopy and photoluminescence measurements. The achievement to introduce Er dopants into ZnO flower-like structures by the time- and cost-effective wet chemical reaction at low temperature for the first time has vast potential to scale up for possible applications. The photoluminescence properties are significantly improved compared to that reported in the literature for the Er-doped nanowires and thin films and shall be much more applicable in optical and communication devices. The flower-like structures are expected to be advantageous in serving as a multi-directional infrared emitters and/or detectors.

1 Introduction Zinc oxide, one of the most promising material, has been demonstrated to be applicable in solar cells [1, 2], light-emitting diodes [3, 4], room temperature ultraviolet lasers [5], gas sensor [6], field-effect transistors [7] and piezoelectric-gated diode [8]. It has attracted increasing interest in fabricating ZnO structures with designed morphology and properties while the desired optical and electrical properties could be achieved by doping ZnO with various elements.

Introduction of impurity atoms is the most widely adopted method to tune the magnetic, electrical and optical properties of materials, but doping becomes difficult in aqueous systems because doping species would form metal-aquo complex easily and not merge into the crystal lattice [9]. The Er-doped semiconductors are the potential optoelectronic materials [10–13] due to the Er intra-4f shell transition with a photoemission at a wavelength of 1.54 μm, which lies in the minimum loss region of silica-based optical fibers [10, 14]. Zinc oxide is chosen to be the host semiconductor [15–17], not only due to the wide band gap which can be applicable to the excitation of Er, but also the controllable electrical conductivity [18].

Up to now, physical doping methods, such as ion implantation [19], laser ablation [16], and high temperature calcinations [15, 20], have mainly been used to introduce Er into ZnO substrate, while most researches focused on the formation of films. Recently, Er-doped ZnO nanowires have been fabricated using Er-ion implantation [19]. However, a high density of defects, such as end-of-range (EOR) defects [21], were formed in the ion-implanted samples. The defects are detrimental to device applications but persist even after annealing at high temperature for a long time.

Herein, we report a facile method for the fabrication of single-crystal Er-doped ZnO structures in large scale

based on hydrothermal process to introduce Er into ZnO structures. Compared to physical doping methods, hydrothermal method are advantageous for low reaction temperature, low cost, minimum equipment requirement, atmospheric pressure and product homogeneity [9, 23–25]. In addition, doping species will fill into the whole structure and not only on the surface. The proper reaction conditions to grow Er-doped ZnO flower-like structures were found to be very constricted by varying the concentration of reactants, additive amount of base and Er salt, species of mineralizers as well as reaction temperature and time.

2 Experimental The growth on Si wafer was carried out using a hydrothermal process. Si wafer (001) was cut into 1×1 cm^2 slices as substrates and then cleaned ultrasonically for 10 min in acetone. All chemical reagents utilized in the present study were of analytical grade (AR) and used without further purification. A thin film of zinc acetate was spin coated on the substrate with a solution containing 5 mM zinc acetate dihydrate (98%, Aldrich) added to the ethanol for 10 times. ZnO films of 5–10 nm thickness were produced after annealing at 300 °C in air for 20 min [9]. ZnO flower-like structures were grown by an aqueous chemical method in 100 ml of aqueous solution containing 10 mM zinc nitrate hexahydrate (98%, Aldrich) and 2.5 ml ammonia solution (28%, Showa). The substrate was positioned at the bottom of the beaker and heated to 90 °C or for 2 h. On the other hand, Er-doped ZnO flower-like structures were formed under the same reaction condition with extra amount (443.4 mg) of erbium nitrate pentahydrate (99.9%, Aldrich) added into solution. The products on Si wafer were cleaned with deionized water and than dried in an air atmosphere.

The ZnO structures were examined with a field emission scanning electron microscope (FESEM) using a JEOL JSM-6500F SEM operating at 10 kV accelerating voltage. The cathodoluminescence (CL) spectra were acquired with an electron probe microanalyzer (Shimadzu EPMA-1500) attached to an SEM. CL spectra were acquired in a single shot mode within an exposure rate of 2 nm/s and were taken at room temperature. A JEOL-2010 transmission electron microscope (TEM) operating at 200 kV was used to examine the microstructures. An electron dispersive spectrometer (EDS) attached to the TEM was used to determine the composition of flower-like structures. The X-ray diffraction (XRD) spectra were taken for phase identification with a Shimadzu 6000-XRD with Cu K_α radiation ($\lambda = 0.154$ nm). Photoluminescence (PL) properties were measured at room temperature with a He–Cd laser as the excitation source. The collected luminescence was dispersed by a 0.19 m monochromator equipped with a 600 gr/mm grating, and was detected by a extended InGaAs detector (cutoff wavelength 2.4 μm) using a standard lock-in technique. The X-ray photoelectron spectroscopy (XPS) was carried out with an ESCA model PHI 1600 to obtain the binding energy of Er.

3 Results and discussion Figure 1 shows XRD patterns of the samples with and without Er-doping. All the diffraction peaks can be indexed to those of Wurtzite (hexagonal) ZnO structure and the sharp diffraction peaks indicate the good crystallinity of the as-synthesized products. The differing of relative intensities of the peak from the standard pattern of the bulk material is caused by preferred orientation and distribution of the ZnO crystals on the substrate surface [26]. It is worth mentioning that no Er_2O_3 diffraction peaks were observed in the XRD patterns indicating the absence of Er_2O_3 either on the ZnO surface or in the ZnO structures.

Figure 2 shows the XPS spectra which disclose the binding state of the compositional elements. The Er 4d peak of the Er-doped ZnO flower-like structures is observed at 170.8 eV. For the pure ZnO flower-like structures, no signals at this region are detected in the spectrum. The result suggests the oxidized state of Er in ZnO flower-like structures and indicates the existence of Er within flower-like structures. It is worthwhile to mention that because of the instrumental limitation, the two peaks which stand for Er $4d_{3/2}$ (176.7 eV) and Er $4d_{5/2}$ (167.6 eV) can not be resolved.

The morphology of the as-synthesized products has been examined by SEM. The general morphologies of pure and Er-doped ZnO flower-like structures are similar, as shown in Fig. 3(a) and (b). The pure ZnO flower-like structures appear to grow with more petals than Er-doped ones. The density of ZnO flower-like structures decreases when equimolar erbium nitrate pentahydrate was added. Each petal of ZnO flower-like structures is a needle-like rod, which is grown from the core of flower-like structures.

A TEM image is shown in Fig. 3(c). The diameter and the average length of individual petals vary in the range of 300–600 nm and 2–3 μm, respectively. The Er-doped ZnO flower-like structures are uniformly spread on Si susbtrate and can be prepared in large quantity in a short period of time. Figure 3(d) shows a high-resolution TEM (HRTEM) image taken from a petal of Er-doped flower-like structure. The corresponding selected area electron

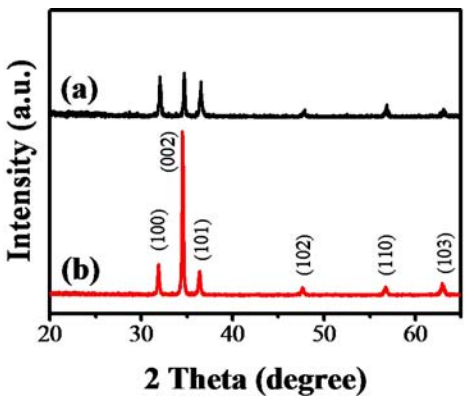

Figure 1 (online colour at: www.pss-a.com) XRD patterns of (a) pure ZnO and (b) Er-doped ZnO flower-like structures.

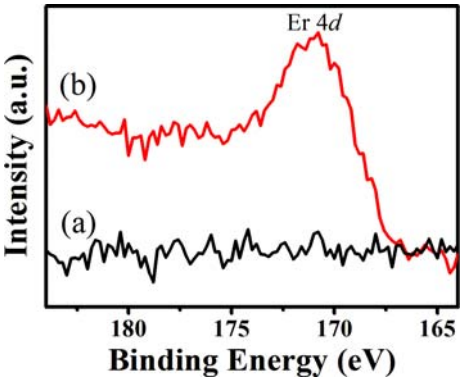

Figure 2 (online colour at: www.pss-a.com) XPS spectra of Er 4d band of (a) pure ZnO and (b) Er-doped ZnO flower-like structures.

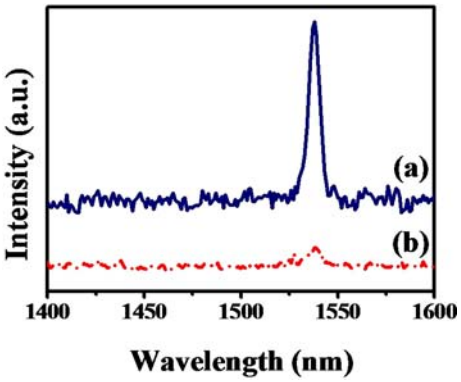

Figure 4 (online colour at: www.pss-a.com) Room-temperature PL spectra of (a) as-synthesized Er-doped ZnO flower-like structures and (b) Er_2O_3 standard.

diffraction (SAED) pattern, shown in the inset of Fig. 3(d), indicates that it is of single-crystal structure with [001] growth direction. The Er L edge and M edge signals in EDS spectra disclose the existence of Er atoms, as shown in Fig. 3(e). The average local Er concentration was found to be about 2.12%. In addition, when focusing the electron probe on the edges of petals of Er-doped flower-like structures, there were no polycrystalline Er_2O_3 layers or grains found in the SEM images. In the corresponding SAED, no rings which could be ascribed to Er_2O_3 grains on the surface were observed. The results from TEM analyses are consistent with XRD as well as XPS data and further confirmed that Er atoms have been incorporated into ZnO lattice but not attached on the surface of ZnO structures.

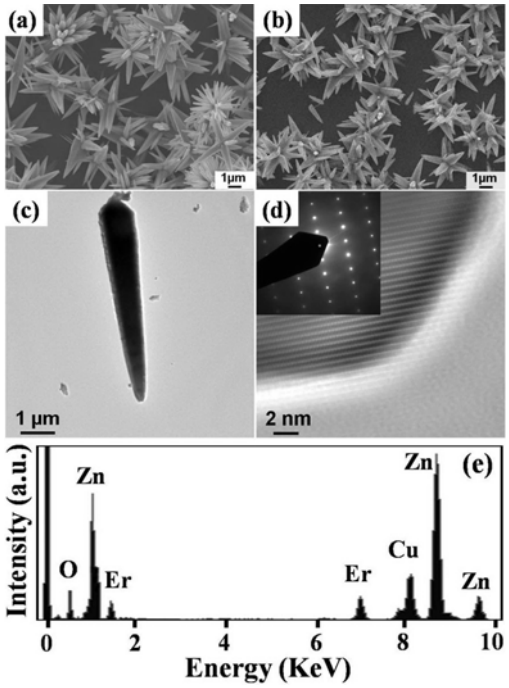

Figure 3 (a) SEM image of ZnO flower-like structures on Si substrate. (b) SEM image of Er-doped ZnO flower-like structures on Si substrate. (c) TEM image of Er-doped ZnO flower-like structures. (d) SAED pattern and HRTEM image revealing the single crystallinity and [001] growth direction of a ZnO petal. (e) EDX spectrum taken from the middle region of a petal.

The PL spectra of Er-doped ZnO flower-like structures and Er_2O_3 powder are shown in Fig. 4. A peak centered at 1540 nm was observed corresponding to the intra-4f shell transition. The Er emission mechanism is through the generation of electron–hole pairs under irradiation of laser beam, and the absorbed energy is then transferred to Er^{3+} ions [10]. The desired 1.54 μm emission comes from the relaxation of Er^{3+} ion from the metastable state ($^4I_{13/2}$) to the ground state ($^4I_{15/2}$). As shown in Fig. 4, a weak and a very strong peaks around 1.54 μm were caused by the Er_2O_3 standards and Er-doped ZnO flower-like structures, respectively. The intense and sharp peak of Er-doped ZnO flower-like structures reveals a successful Er-doping in ZnO and, at the same time, not through the formation of erbium oxide.

The full width at half maximum (FWHM) of 1.54 μm peak for Er-doped ZnO flower-like structures was measured to be 5.9 nm. This compares favorably with a value of 48.6 nm for Er-ion implanted ZnO nanowires reported in the literature for the only other Er-doped nanowire work [19] as well as Er-doped ZnO thin films [16, 20]. The much narrower 1.54 μm peak of Er-doped flower-like structures is attributed to the absence of structural defects. Distinct defects caused by ion-implantation were observed in TEM images and these defects are detrimental to the PL properties. Furthermore, the defects could not be completely removed even after annealing at 800 °C for 1 hr [19]. On the other hand, the Er-doped ZnO flower-like structures synthesized by low temperature hydrothermal method are essentially free from structural defects. The significantly narrower (less than one-eighths) FWHM of PL peak of Er-doped ZnO flower-like structures shall be much more applicable in optical and communication devices.

The formation of Er-doped ZnO flower-like structures is proposed to follow the series of chemical reactions:

$$NH_3 \cdot H_2O \rightarrow NH_4^+ + OH^- , \quad (1)$$

$$Zn^{2+} + 4NH_3 \cdot H_2O \rightarrow Zn(NH_3)_4^{2+} + 4H_2O , \quad (2)$$

$$Zn(NH_3)_4^{2+} + 2OH^- \rightarrow ZnO + 4NH_{3\uparrow} + H_2O . \quad (3)$$

In solution, the formation of ZnO structures is through the nucleation and growth process. When zinc nitrate pentahydrate was dissolved into DI water, the zinc cations were formed. The combination of zinc and ammonia results in the $Zn(NH_3)_4^{2+}$ complex which is likely to be the active site of growth. The fast nucleation of ZnO leads to more nucleation sites. The nuclei agglomerated under supersaturation. To minimize surface energy, each of them grows along the *c*-axis from the circumference of ZnO core, and the flower-like structure composed of rods is constructed [25, 27].

The morphology and property of synthesized products can be substantially changed by fine tuning the condition of reaction, such as the pH value, temperature and concentration of reactants. The concentrations of zinc nitrate hexahydrate and erbium nitrate pentahydrate were found to be critical parameters in affecting morphology. The best condition, which introduced Er into ZnO lattice and maintained the structure of flower-like structures, was achieved when equimolar Er and Zn sources were added into solution (both Zn and Er source are 10 mM in solution). When the concentration of $Er(NO_3)_3$ is reduced to half of $Zn(NO_3)_2$, Er barely fills into ZnO lattice. Only trivial value of Er was detected in EDS. In contrast, excess amount of $Er(NO_3)_3$ would severely etch the surface of flower-like structures. When the amount of erbium source was twice of that of zinc source, 4.96 at% Er atoms were found to dope into ZnO from the EDS detection. At this condition, although the flower-like structures remained, all petals were severely etched (not shown). When the quantity of $Er(NO_3)_3$ was much more than zinc source e.g. the concentration of $Er(NO_3)_3$ was more than three times of that $Zn(NO_3)_2$, mostly non-uniform film on Si wafer instead of a high density of flower-like structures was formed (not shown).

The amount of ammonia, a weak base with 4.75 pKb value, also plays an important role in the reaction. Ammonia affects the products of reaction in two major aspects [22]. During reaction process, ammonia serves as a complex agent, which forms the $Zn(NH_3)_4^{2+}$ complex with zinc ion. In addition, the pH value of aqueous solution is adjusted by the hydrolysis of ammonia. The flower-like structures were formed due to the coordination of ammonia on ZnO crystal and hindrance of the growth on some surface [9]. With increasing concentration of ammonia in reaction, the density of product decreased and each petal grew thinner and longer in appearance, as shown in Fig. 5. Furthermore, Er was only detected by EDS in the samples synthesized with 2.5% ammonia.

In wet chemical reactions, mineralizers are key factors to determine the morphology of products. Various mineralizers, for example hexamethylenetetramine (HMTA), 1,3-diaminopropane (1,3-DAP) and ammonia were examined in reactions, as shown in Fig. 6. While different morphologies accompany varied mineralizers, Er signal was only detected by EDS in samples prepared with ammonia as the mineralizer. The results indicate that the NH_3 ligands play an important role in the formation of Er-doped ZnO flower-like structures. The Er^{3+} anion might form complex with ammonia in solution. When appropriate amount of $Er(NH_3)_x^{3+}$ complex was present in solution, with the heating and stirring, the complex might play the role to provide Er source during the growth of Er-doped ZnO flower-like structures. On the other hand, HMTA and 1,3-DAP might not possess the similar reactivity with Er^{3+} under the same reacting condition. Furthermore, three kinds of seed layers prepared by spin coating with different solution content were tested. However, only the seed layer prepared by 5 mM $Zn(NO_3)_2$ in ethanol produced desired products. After a series of deliberate and systematic attempts, we found that the Er atoms were only introduced into ZnO lattice in a very constricted reaction condition. With careful control over the concentration of Er source and mineralizer as well as seed layer, the Er-doped ZnO flower-like structures were successfully synthesized. The difficulty could be attributed to that doping atoms would easily form aquo ions but not be incorporated into the crystal lattice [9].

A widely adopted model was proposed by Ishii et al. for explaining the local structure of an optically active cen-

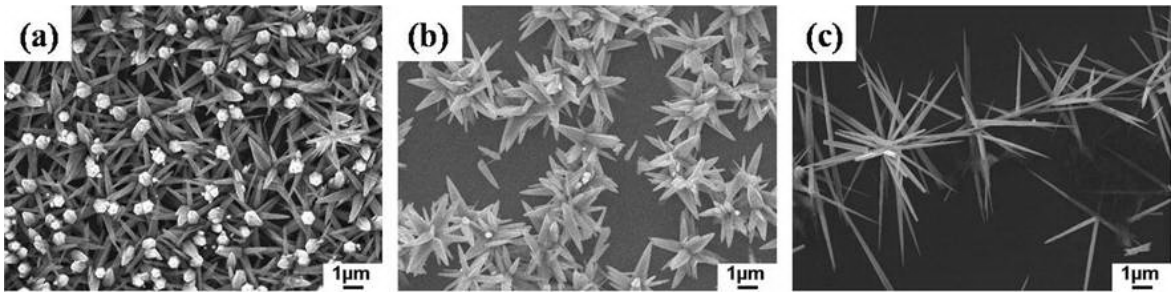

Figure 5 SEM images of ZnO products prepared with different ammonia concentrations at 90 °C for 2 h. (a) 1.5% ammonia, (b) 2.5% ammonia, (c) 3.5% ammonia. Er was only detected by EDS in the samples synthesized with 2.5% ammonia.

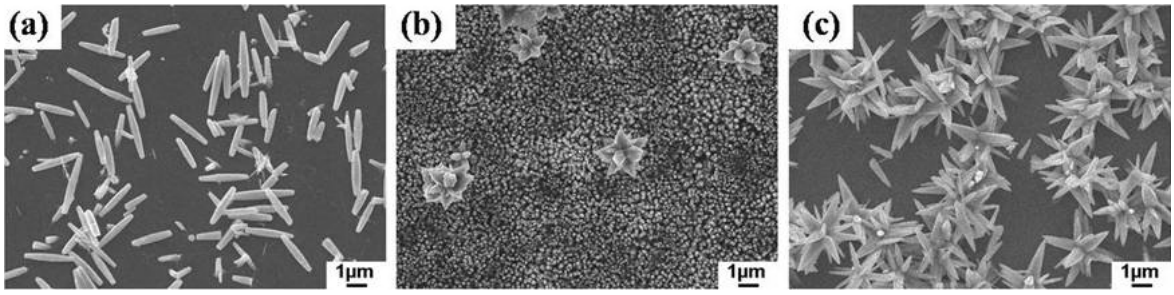

Figure 6 Effects of various mineralizers on the morphology of ZnO structures synthesized by hydrothermal method. (a) Hexamethylenetetramine (HMTA), (b) 1,3-diaminopropane (1,3-DAP), (c) ammonia. Er was only detected in EDS when ammonia serves as a mineralizer.

ter in Er-doped ZnO thin film [17]. The Er atoms introduced into ZnO with physical doping methods, for instance ion implantation and laser ablation, was surrounded by eight oxygen atoms. After annealing, a pseudo-octahedral structure with C_{4v} symmetry is formed due to the resistance of Er–O bond to O diffusion during annealing. In physical doping methods, Er atoms were incorporated into ZnO lattice under an applied force. On the other hand, the detailed route of Er entering into Wurtzite-structure ZnO by low temperature hydrothermal process remained unclear. The present study has demonstrated that the amount of dopant, the characteristic and concentration of mineralizers are the decisive factors for the incorporation of metallic atoms into the lattice of substrate in low temperature aqueous system.

The room-temperature CL was used to characterize the optical properties of ZnO and Er-doped ZnO structures as shown in Fig. 7. The ZnO flower-like structures have an UV emission at 384 nm, which comes from the band edge emission, and a high intensity green emission at 564 nm, attributed to native point defects [28]. The relatively strong green luminescence (about 3 times stronger than ZnO band edge emission) indicates the presence of numerous defects in the flower-like structure. Since the reaction proceeds rapidly in aqueous solution, defects are easily formed in the rapid growth process. The presence of a high density of defects in structures may facilitate the doping of Er into ZnO. The CL spectrum of Er-doped ZnO flower-like structures also revealed that green emission is significantly enhanced (about 8 times stronger than ZnO band edge emission). The increase in native defects can be ascribed to that when Er^{3+} replaces Zn^{2+}, oxygen defects are usually generated to keep the charge neutrality [19]. The enhancement of green emission is therefore correlated well with the successful substitution of Er atoms into Zn sites in the ZnO lattice.

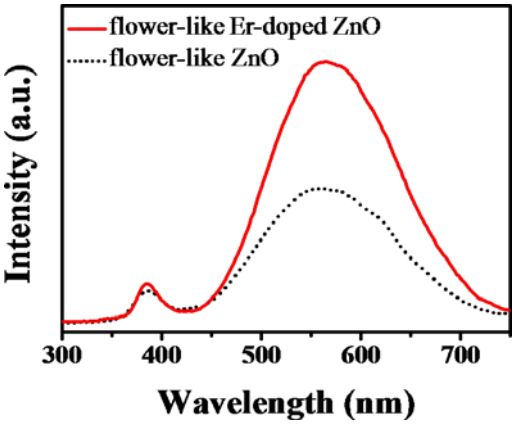

Figure 7 (online colour at: www.pss-a.com) Cathodoluminescence spectra of pure and Er-doped ZnO flower-like structures.

4 Conclusions In conclusion, the synthesis of single-crystal Er-doped ZnO structures by a low-temperature hydrothermal process was achieved for the first time. XRD, ESCA, TEM/EDS and PL all confirmed that Er atoms were incorporated into ZnO lattice. Owing to the difficulty in introducing dopant atoms into crystal lattice in low-temperature wet chemical reaction, the Er-doped ZnO flower-like structures were successfully synthesized only with careful control over the concentration of Er source and mineralizer as well as seed layer. The wet chemical method for doping Er has advantages in low reaction temperature, low cost, minimum equipment requirement and product homogeneity over physical doping methods. The best ever narrow FWHM of 1.54 μm PL peak of Er-doped ZnO flower-like structures shall facilitate their application as multidirectional emitting and/or detection source for infrared optoelectronic devices.

Acknowledgements The research was supported by the National Science Council through grants No. NSC 96-2221-E-007-151 and NSC 96-2120-M-007-006.

References

[1] H. Rensmo, K. Keis, H. Lindström, S. Södergren, A. Solbrand, A. Hagfeldt, S. E. Lindquist, L. N. Wang, and M. Muhammed, J. Phys. Chem. B **101**, 2598 (1997).
[2] M. Law, L. E. Greene, J. C. Johnson, R. Saykally, and P. D. Yang, Nature Mater. **4**, 455 (2005).
[3] D. K. Hwang, S. H. Kang, J. H. Lim, E. J. Yang, J. Y. Oh, J. H. Yang, and S. J. Park, Appl. Phys. Lett. **86**, 222101 (2005).
[4] J. H. He, S. T. Ho, T. B. Wu, L. J. Chen, and Z. L. Wang, Chem. Phys. Lett. **435**, 119 (2007).

[5] M. H. Huang, S. Mao, H. Feick, H. Yan, Y. Wu, H. Kind, E. Weber, R. Russo, and P. D. Yang, Science **292**, 1897 (2001).
[6] H. Kind, H. Q. Yan, B. Messer, M. Law, and P. D. Yang, Adv. Mater. **14**, 158 (2002).
[7] M. S. Arnold, P. Avouris, Z. W. Pan, and Z. L. Wang, J. Phys. Chem. B **107**, 659 (2003).
[8] J. H. He, C. L. Hisn, J. Liu, L. J. Chen, and Z. L. Wang, Adv. Mater. **19**, 781 (2007).
[9] L. E. Greene, B. D. Yuhas, M. Law, D. Zitoun, and P. D. Yang, Inorg. Chem. **45**, 7535 (2006).
[10] A. Polman, J. Appl. Phys. **82**, 1 (1997).
[11] S. Lanzerstorfer, L. Palmetshofer, W. Jantsch, and J. Stimmer, Appl. Phys. Lett. **72**, 809 (1998).
[12] S. Coffa, G. Franzo, F. Priolo, A. Pacelli, and A. Lacaita, Appl. Phys. Lett. **73**, 93 (1998).
[13] X. Zhao, S. Komuro, H. Isshiki, Y. Aoyagi, and T. Sugano, Appl. Phys. Lett. **74**, 120 (1999).
[14] K. Takahei and A. Taguchi, J. Appl. Phys. **74**, 1979 (1993).
[15] N. Mais, J. P. Reithmaier, A. Forchel, M. Kohls, L. Spanhel, and G. Muller, Appl. Phys. Lett. **75**, 2005 (1999).
[16] S. Komuro, T. Katsumata, T. Morikawa, X. W. Zhao, H. Isshiki, and Y. Aoyagi, J. Appl. Phys. **88**, 7129 (2000).
[17] M. Ishii, S. Komuro, T. Morikawa, and Y. Aoyagi, J. Appl. Phys. **89**, 3679 (2001).
[18] J. H. He, C. S. Lao, L. J. Chen, D. Davidovic, and Z. L. Wang, J. Am. Chem. Soc. **127**, 16376 (2005).
[19] J. Wang, M. J. Zhou, S. K. Hark, Q. Li, D. Tang, M. W. Chu, and C. H. Chen, Appl. Phys. Lett. **89**, 221917 (2006).
[20] Z. Zhou, T. Komori, T. Ayukawa, H. Yukawa, M. Morinaga, A. Koizumi, and Y. Takeda, Appl. Phys. Lett. **87**, 091109 (2005).
[21] J. H. He, W. W. Wu, and L. J. Chen, Nucl. Instrum. Methods B **237**, 174 (2005).
[22] Z. Wang, X. F. Qian, J. Yin, and Z. K. Zhu, Langmuir **20**, 3441 (2004).
[23] J. H. He, J. H. Hsu, H. N. Lin, L. J. Chen, and Z. L. Wang, J. Phys. Chem. B **110**, 50 (2006).
[24] Y. C. Chang and L. J. Chen, J. Phys. Chem. C **111**, 1268 (2007).
[25] H. Zhang, D. Yang, X. Y. Ma, Y. J. Ji, J. Xu, and D. L. Que, Nanotechnology **15**, 622 (2004).
[26] T. Andelman, Y. Gong, M. Polking, M. Yin, I. Kuskovsky, G. Neumark, and S. O'Brien, J. Phys. Chem. B **109**, 14314 (2005).
[27] W. Q. Peng, S. C. Qu, G. W. Cong, and Z. G. Wang, Cryst. Growth Des. **6**, 1518 (2006).
[28] K. Vanheusden, C. H. Seager, W. L. Warren, D. R. Tallant, and J. A. Voigt, Appl. Phys. Lett. **68**, 403 (1996).